Поляризационные радары с фазированной антенной решеткой для метеорологических наблюдений: состояние и проблемы.

Д. Миркович[(1)] и Д. Зрнич[(2)]
[(1)]Университет Оклахомы, США
[(2)]Национальная лаборатория по исследованию сильных штормов, США, 120 David L Boren Blvd, Norman, Oklahoma, USA, 73072.

В докладе содержится краткий обзор исследований направленных на разработку и калибровку нового поколения метеорологичесих поляризационных радаров с фазированной антенной решеткой. В частности, обсуждаются вычислительные методы электродинамики для расчета разности фаз и усиления между сигналами с ортогональными поляризациями излучаемыми антенной с фазированной решеткой.

Polarimetric phased-array radar for weather observations: status and challenges

Djordje Mirkovic[1,2], Dusan Zrnic[2]
[1]University of Oklahoma (CIMMS),
[2]National Severe Storms Laboratory (NOAA)
Norman, Oklahoma, USA
Djordje.Mirkovic@noaa.gov

A short overview of current research in development and calibration for the new generation of polarimetric phased array weather radars (PPAR) is presented. Specifically the use of computational electromagnetic (CEM) tools to infer the differential phase and gain between signals at two orthogonal polarization of a PPAR antenna is illustrated.

1. Introduction

Radars with phased array antennas were developed by the military to track multiple targets [1]. Their beams have no mechanical inertia and can be positioned extremely fast. The speed depends on the time it takes to switch the phases of the antenna elements. Electronic scanning eliminates moving parts and inertial constraints of dish antennas.

Exploiting application of this technology to weather observation is nascent whereas its use in tactical missions has a history of few decades. Yet, there are compelling scientific and practical reasons to rapidly acquire volumetric radar data. Features such as adaptive scans, faster scans, the absence of beam smearing and adaptive (quick) change of signal transmission/reception modes could be beneficial to observations of weather [2]. There is potential, with quicker observations to increase the tornado warning lead time beyond the present 10 to 15 minutes. Claims have been made that adaptive scans combined with adaptive signal design and processing could make possible observations of winds and humidity in clear air around storms. It has also been suggested that this versatility would enable the PARs to fulfill two missions, tracking of aircraft needed by controllers and observing weather [3]. The two missions can be naturally interleaved near airports where both detecting weather hazards and managing air traffic are most critical.

2. Configuration of PAR antennas

The following three PAR antenna configurations have been proposed and/or explored for weather observations. 1) A panel antenna (Fig. 1a) can be mounted on a mechanically steerable platform. One such example is the mobile, X-band, radar combining electronic scanning in elevation with mechanical in azimuth [4]. Another is also X-band but with mechanical scanning in elevation and electronic in azimuth [5]. 2) Multiple panel (typically four) antenna [1]. 3), Fig. 1b. Cylindrical antenna [6, 7], (Fig. 1c). Each of these can cover the volume quicker than a mechanically steered beam due to beam agility, versatility in beam construction, shape, and speed of changing pointing direction.

Semi coherency of weather returns imposes a fundamental limitation on the dwell time needed to obtain estimates of radar variables with sufficient accuracy. Any radar including the PAR is up against this constraint. The PAR's advantage is its beam agility. Thus multiple beams truly in parallel (for example from a four panel array one beam per panel) can be transmitted. A very wide beam can be transmitted but several narrow beams can be synthesized to simultaneously sweep a large spatial volume [3]. Or, in a shot gun approach a transmitted pulse can be subdivided into chunks (sub pulses) each of which is sent to a separate direction to probe these simultaneously [8]. Beam agility enables adaptive scans to be directed into regions of hazardous weather for fast updates [9]. Which of these volume coverage accelerators is best suited for weather PAR is subject of current studies.

Achieving comparable or better accuracy in the polarimetric variables than on the US national network of weather radars, WSR-88D, is challenging to all three PAR configurations. It is most difficult for the planar PAR with multiple faces. This is because it is complicated to generate orthogonal electric fields at all pointing directions, as explained next.

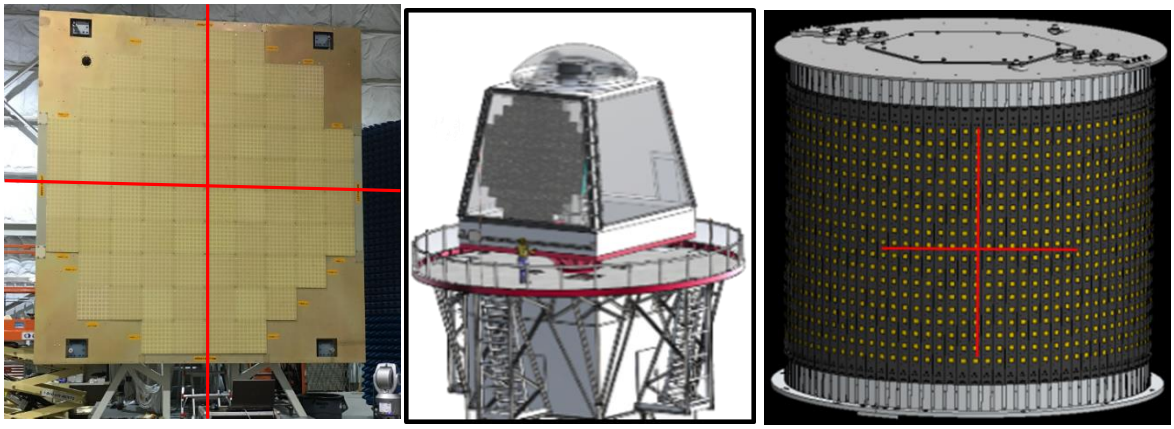

(a) **(b)** **(c)**

Fig. 1. a) Planar array antenna. It consists of 76 panels (light colors) each with 64 radiating elements. It has dual polarization. The antenna has been mounted on a rotating platform and is part of the Advanced Technology Demonstrator for weather observations. The red lines indicate the principal planes. b) Sketch of four planar antennas mounted on a fixed platform. This arrangement enables fully electronic scanning in all directions. (c) Cylindrical PAR developed by the University of Oklahoma [10]. The beams are scanned electronically in elevation and commute in azimuth

Imagine an array panel centered in a globe (Fig.2). The meridians and parallels of the globe intersect at right angles. Thus, the planar antenna should generate electric fields tangent to the latitude circles (i.e., intended horizontal polarization) and tangent to the meridian circles (i.e.,

intended vertical polarization). This is in principle possible if the radiators for the horizontal polarization are magnetic dipoles and radiators for the vertical polarization are electric dipoles [11]. Such configuration has yet to be tested on a real PAR. If successful, then to become operational manufacturing at an affordable price would need to be developed.

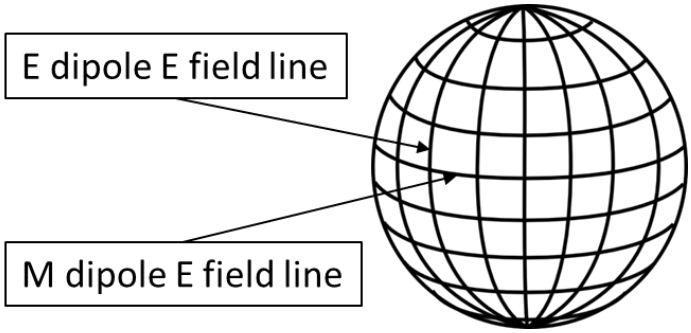

Fig. 2. Depiction of a globe illustrating the desirable orthogonal fields. The H filed is directed along parallels and the V along meridians. The antenna is located in the globe center

The dual polarization PARs have the same type of radiators for "horizontal" and "vertical" polarization. Therefore, the transmitted E fields are only orthogonal in the two principal planes of the array. One is the horizontal plane perpendicular to the array face; the other is the vertical plane perpendicular to the array face. In other directions the electric fields are not orthogonal, although for patch antennas (the ones currently used on experimental PARs) the "intended horizontal" field is indeed horizontal. The intended vertical field is at an angle with respect to the meridian causing coupling with the horizontally polarized field. The coupling appears as a cross-polar beam (collinear with the copolar beam). It is referred to as "geometrically induced". It depends on the pointing direction, and must be accounted for. Moreover, the gains and beamwidths depend on the pointing direction.

3. Effects of copolar and cross-polar patterns on polarimetric variables

For polarimetric variables defined as in [12] and for a single spherical scatterer we can express the return voltage as,

$$\begin{vmatrix} \delta V_{\mathrm{h}} \\ \delta V_{\mathrm{v}} \end{vmatrix} \equiv \vec{V} = \mathbf{F}^{t}\mathbf{S}\mathbf{F}\vec{W}_{\mathrm{i}} = \begin{vmatrix} F_{\mathrm{hh}} & F_{\mathrm{vh}} \\ F_{\mathrm{hv}} & F_{\mathrm{vv}} \end{vmatrix} \begin{vmatrix} s_{\mathrm{hh}} & 0 \\ 0 & s_{\mathrm{vv}} \end{vmatrix} \begin{vmatrix} F_{\mathrm{hh}} & F_{\mathrm{hv}} \\ F_{\mathrm{vh}} & F_{\mathrm{vv}} \end{vmatrix} \vec{W}_{\mathrm{i}}, \tag{5}$$

where the transmitted voltage $\vec{W}_{\mathrm{i}}$ produces either H ($\vec{W}_{\mathrm{i}} = |1,0|^{T}$) or V($\vec{W}_{\mathrm{i}} = |0,1|^{T}$) polarizations which could alternate from pulse to pulse in the so called Alternate Horizontal and Vertical (AHV) mode, or be fixed. If $\vec{W}_{\mathrm{i}} = |1, e^{j\beta}|^{T}$ then the polarimetric mode is SHV (simultaneous) which has been a choice on radars with dish antenna. The angle β is the differential phase on transmission. The superscript "T" denotes the transpose matrix. F_{hv} is proportional to the H radiated electric field if the V channel is excited, and vice versa holds for F_{vh}. The copolar (one-way voltage) pattern functions F_{ii} are not normalized but contain the peak power gain g_{ii} so that

$$F_{\mathrm{ij}}(\theta,\phi) = \sqrt{g_{\mathrm{ij}}}\, f_{\mathrm{ij}}(\theta,\phi). \tag{6}$$

Furthermore, the proportionality constants in (5) to make it dimensionally correct are implicit. The angles (θ, ϕ) are relative to the copolar beam axis. It is further stipulated that within the main beam F_{hh} and F_{vv} are real function (i.e., with zero reference phase), but F_{hv}, F_{vh} are complex.

By integrating the powers and correlations from (5) over the main beam and in the SHV or AHV modes one can obtain the polarimetric variables under conditions suitable for quantitative assessment of the pattern effects. For example, one can assume same type of scatterers that produce fixed differential reflectivity and determine what the effects of patterns are. In doing so it turns out the biases depend on the values of the polarimetric variables including the one being assessed. Nonetheless it is possible to determine the worst case (combination of variables) that produces larges bias for each variable.

3.1 Effects of cross-polar patterns

Coupling effects on the polarimetric variables differ substantially in the two modes. A heuristic explanation with the aid of Fig. 3 follows. In the alternate mode if the port for the H field is exited the forward propagating field along a path is proportional to $F_{hh}\hat{\boldsymbol{h}} + F_{vh}\hat{\boldsymbol{v}}$ (where the unit vectors are orthogonal and the coupling from H to V is quantified with F_{vh}. This field upon reflection from a perfect sphere would retain the same relative strengths of the two orthogonal components. At the antenna output corresponding to the H component the signal is proportional to $F_{hh}^2 + F_{vh}F_{hv}$ in which the second term results from the coupling (V to H). The power δP_{hh} along a ray is proportional to

$$\delta P_{hh} \propto F_{hh}^4 + 2\,\mathrm{Re}(F_{hh}^2 F_{vh} F_{hv}) + |F_{vh}F_{hv}|^2 . \qquad (7)$$

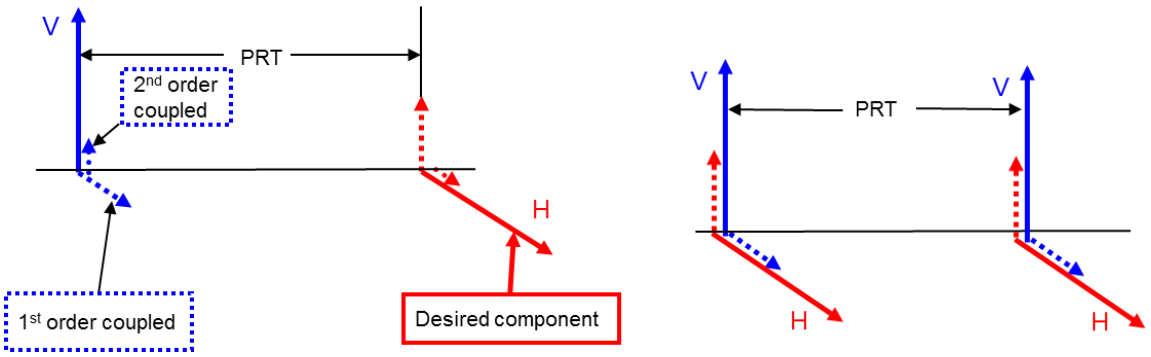

(a) **(b)**

Fig. 3. a) Time-space depiction of two consecutive pulses in the alternate mode of Horizontal and Vertical transmission (AHV). The vertically polarized transmitted filed is indicated with the blue vertical (full) line. It couples into the horizontal polarization (horizontal dashed line). After reflection the horizontal (coupled component) couples back to the vertical (dashed short vertical blue line). The net effect at the receiver is second order. Similar coupling happens to the horizontally polarized field of the second pulse (red full horizontal line). b) Same as in a) but the simultaneous mode of Horizontal and Vertical transmission (SHV) is used. Both field components are transmitted simultaneously. Therefore, the resulting polarization is elliptical, but the strengths of each component must be known for computing the polarimetric variables. Because strong components are also received simultaneously first order coupling is present in each and it is much stronger than the second order coupling.

This is valid at every ray within the beam but the values of the pattern functions F_{ij} depend on the location within the beam. Integration of (7) over the beam (solid angle Ω) produces the total power $P_{hh} = \int_{\Omega} \delta P_{hh} d\Omega$. Differential reflectivity and correlation coefficient are obtained from the powers and cross correlations. The unbiased differential reflectivity is proportional to $\int_{\Omega} F_{hh}^4 d\Omega / \int_{\Omega} F_{vv}^4 d\Omega$. The coupling contribution comes from the terms with $F_{hv}F_{vh}$ and obviously the contribution by $2\,\mathrm{Re}(F_{hh}^2 F_{vh} F_{hv})$ is much larger than the one by $|F_{vh}F_{hv}|^2$.

For the SHV mode (Fig. 6) we follow the same arguments that lead to (7) and express the returned total power as

$$P_{hh} \propto \int_{\Omega} \left[F_{hh}^4 + 2\,\mathrm{Re}(F_{hh}^3 F_{hv}) + |F_{hh}F_{hv}|^2 \right] d\Omega . \tag{8}$$

But now the largest bias term is $2\int_{\Omega} \mathrm{Re}(F_{hh}^3 F_{hv}) d\Omega$ because it has the cross pattern function F_{hv} raised to the first power.

In the SHV mode the value [13] and (Galletti and Zrnic)

$$W_{hv} = \int_{\Omega} F_{hh}^3 |F_{hv}| d\Omega / \int_{\Omega} F_{hh}^4 d\Omega \ , \tag{9a}$$

and

$$W_{vh} = \int_{\Omega} F_{hh}^3 |F_{vh}| d\Omega / \int_{\Omega} F_{hh}^4 d\Omega \ , \tag{9b}$$

determine the first order (in F_{ij}) bias in all three polarimetric variables. Clearly the shape and phases of the cross-polar (voltage) patterns F_{hv}, F_{vh} are crucial. Cross-polar patterns on broad side (Fig. 5) have four symmetric peaks with alternating phase and therefore the terms (9a, b) are zero and only second order terms cause bias. Cross-polar patterns of beams pointing along the principal planes have two peaks with alternating sign and these also cancel in the integrals (9). Some examples of the PAR patterns are in the next section.

If (9a and 9b) are zero, the second order terms cause bias in the SHV mode. The relative value of the second order term is

$$W = \int_{\Omega} F_{hh}^2 |F_{hv}^2| d\Omega / \int_{\Omega} F_{hh}^4 d\Omega \ . \tag{10}$$

It can be shown [13] that the lower limit of linear depolarization ratio due to the cross-polar contribution by the antenna is

$$\sup \min(L_{dr}) = 4 \int_{\Omega} F_{hh}^2 |F_{hv}|^2 \, d\Omega / \int_{\Omega} F_{hh}^4 \, d\Omega \tag{11}$$

In the AHV mode the first order term does not appear and the second order term (10) is the dominant contributor to bias.

From the expositions so far it is clear that the copolar pattern matching is important for precise measurements of correlation and that the terms (9) and (10) must be small to reduce bias in the polarimetric variables. The values of these terms depend heavily on the cross-polar pattern. Determining these patterns with the precision required for weather observations is needed and the following techniques are under investigation. Near field measurements of the current distributions with probes close to the array. Far field measurements. Full modeling of the antenna with computational electromagnetics tools to obtain the patterns. These are complimentary and may supplement each other.

3.2 Main beam shapes and pointing direction

If the beams are not matched in width and/or pointing direction the polarimetric variables can be biased. This happens to all the polarimetric variables if the intrinsic reflectivity changes over the beam. If the reflectivity is uniform over the beam, then only the correlation coefficient would be affected by mismatch of beamwidth and/or pointing direction at the two polarizations.

The biases can be computed from the basic equation expressing the correlation coefficient as

$$\rho_{\mathrm{hv}} = \frac{\int_{\Omega} F_{\mathrm{hh}}^2 F_{\mathrm{vv}}^2 d\Omega}{\left(\int_{\Omega} F_{\mathrm{hh}}^4 d\Omega\right)^{1/2} \left(\int_{\Omega} F_{\mathrm{vv}}^4 d\Omega\right)^{1/2}}. \tag{12}$$

For narrow beams the area within the solid angle can be replaced with a rectangle in which the coordinate x is along ϕ direction and the coordinate y is along the θ. Assuming a beam center displacement Δ_x, Δ_y and elliptical beam cross sections widths σ_{hx} and σ_{hy} for the H pattern and σ_{vx} and σ_{vy} for the V pattern the correlation coefficient becomes.

$$\rho_{\mathrm{hv}} = \frac{2\sigma_{hx}\sigma_{vx}}{\sigma_{hx}^2 + \sigma_{vx}^2} \exp\left(-\frac{\Delta_x^2}{4(\sigma_{hx}^2 + \sigma_{vx}^2)}\right) \frac{2\sigma_{hy}\sigma_{vy}}{\sigma_{hy}^2 + \sigma_{vy}^2} \exp\left(-\frac{\Delta_y^2}{4(\sigma_{hy}^2 + \sigma_{vy}^2)}\right). \tag{13}$$

The beam cross section width σ is defined as sigma width of two way power pattern and is related to the one way 3 dB beamwidth θ_1 as $\sigma^2 = \theta_1^2 / 16 \ln 2$.

Assuming various degrees of beam mismatch in (13) one can compute the concomitant bias. Perfectly spherical scatterers (like very small drops) produce a correlation equal one and the decrease can be cause by the antenna or the rest of the radar. If the tolerable decrease is less than say 0.995 the value of (13) should be between 0.995 and 1. From this reasoning one can determine the acceptable mismatch of beams.

Equation (13) assumes elliptical beam cross section whereby the axes of the ellipse are aligned with the two orthogonal directions perpendicular to the beam axis. The beam cross sections of planar phased array antennas (of roughly circular shape) are ellipsoidal (except at broadside) and the axis lengths as well as orientation depend on the pointing direction. Determination of the shapes of the beam is important for accurate computation of the reflectivity. Matching is required to produce good quality polarimetric data. The reader can see that (13) can easily be applied to all

orientation by aligning the *x* and *y* coordinates with the axis of the beam cross sections. But establishing the actual mismatch of the H and V beams' cross-sections and pointing directions may be very hard. So here for answers one can resort to computational electromagnetics (CEM) software.

4. Computational Electromagnetics (CEM)

Patterns of phased array antennas can be measured in the far field and near field. Both require special arrangements including access to an antenna range or sophisticated mechanisms for mounting probes in front of the antenna. Furthermore, measurements in all pointing directions would be extremely time consuming. Note, that for each pointing direction two copolar and two cross-polar patterns need to be measured. Therefore, in practice such measurements are made at select directions like broadside, few in principal planes and few out of principal planes. If the results meet expectations, it can be assumed that they will be satisfactory at other pointing directions. Extension to the other directions is a subject of current research.

Computational Electromagnetics (CEM) can supplement the physical measurements and/or yield physical insights without the need to make changes on the antenna. Furthermore, CEM tools can accurately model both, copolar and cross-polar properties of radar antennas [14]. Based on the CEM simulations, biases in the polarimetric variables caused by the antenna can be determined.

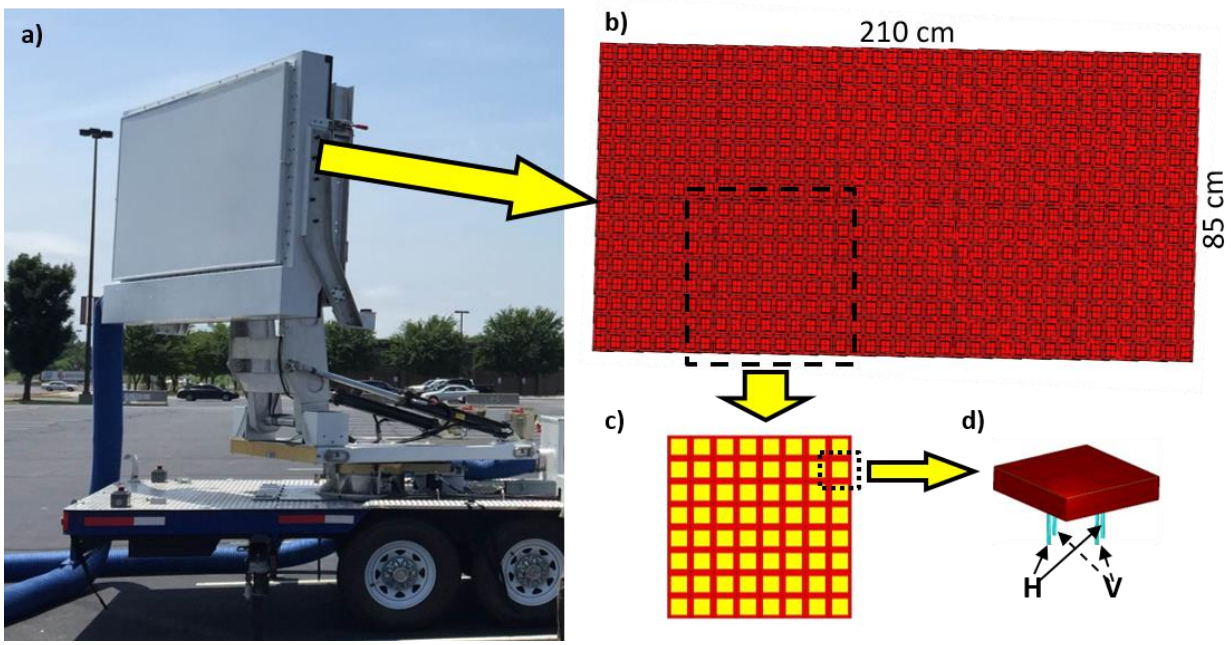

Fig. 4. a) The Ten Panel Demonstrator radar. b) The antenna model. c) The antenna panel (8x8 elements). d) The antenna element with four differentially fed probes.

To illustrate CEM application to polarimetric weather radar calibration we chose the WIPL-D Pro software [15]. The WIPL-D software uses the method of moments and integral equations to simulate large EM structures. We have applied it to the Ten Panel Demonstrator (TPD). This radar has 640 radiating elements, operates at the S band and served as a developmental system on which the phased array technology was tested prior to building the Advanced Technology Demonstrator (ATD with 4863 radiators). The ATD has been installed in Norman OK, USA and is undergoing engineering evaluation at the time of this writing. In Fig.4 are the TPD radar (Fig. 4a), the modeled

antenna array (Fig. 4b), the single panel of the TPD (Fig. 4c) and the single element of the array with differential feeding probes for horizontal (H) and vertical (V) polarization (Fig. 4d). Patterns for all the models (structures) in Fig. 4 are simulated using the WIPL-D solver.

In the antenna model (Fig. 4b) each element of the array can be individually set, enabling evaluation of polarimetric biases at different pointing direction. This is done by adjusting the phases on the element on four ports (Fig. 4d). Consequently, we obtain copolar and cross-polar radiation patterns in the Ludwig 2 definition (L2), [16]. The L2 is the coordinate system of choice due to its use in weather radar [7]. The broadside copolar and cross-polar radiation patterns are presented in Fig. 5.

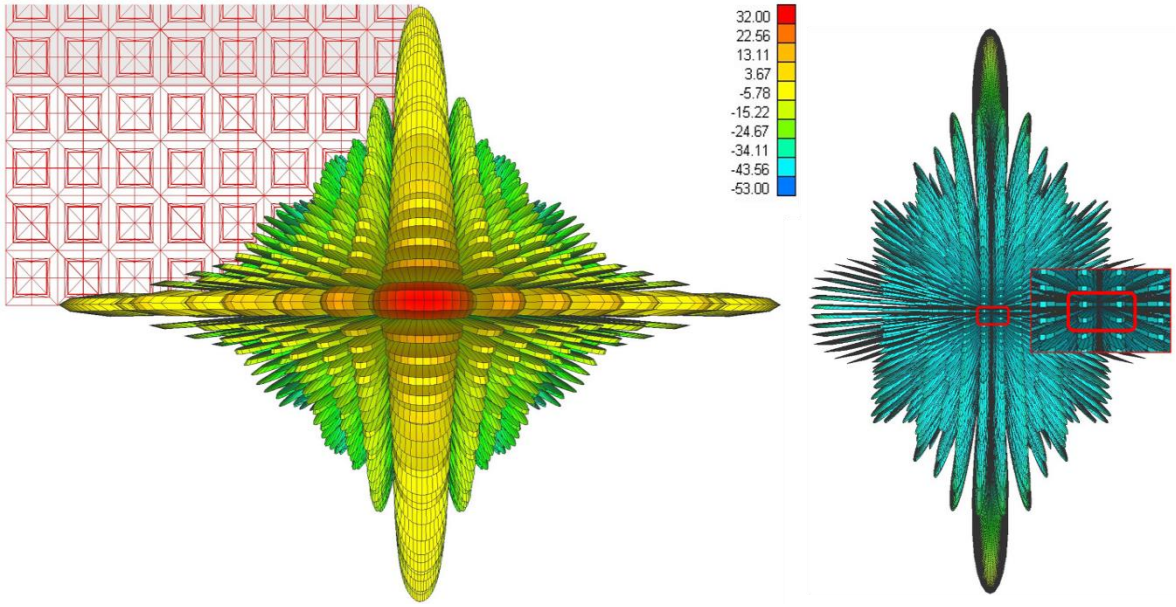

Fig. 5. Antenna patterns of the ten panel demonstrator, left) copolar $f_{hh}(\theta, \phi)$, right) cross-polar $f_{vh}(\theta, \phi)$ and its enlarged values within the main beam (encompassed with the rectangle). The beam is pointing broadside. The peak to peak isolation within the main lobe is over 50 dB while the cross-polar minimum is aligned with the copolar peak. The color bar indicate values in dB

The broadside pattern exhibits expected characteristics with symmetric side-lobes. The beamwidths are: 6.7^o in horizontal (azimuth) direction and 2.6^o in elevation. The most significant, for weather radar application, are properties of the cross-polar radiation pattern within the main lobe. The cross-polar pattern in Fig. 5 has four symmetrically placed lobes with respect to the copolar beam center. This is beneficial as the contribution to the signal from these lobes, due to their opposite phases, cancel out the first order bias term in polarimetric variable.

If the TPD's copolar peak is pointed at 35^o away from broadside in the horizontal principal plane the cross-polar lobe formation changes from the one in Fig. 5. Four symmetric lobes transform into two lobes which have opposite phase. This feature also cancels the first order bias term in the polarimetric variables.

If the beam is steered away from the principal planes (for example at ϕ = 28^o, θ = 14^o), the cross-polar lobe formation changes significantly. The cross-polar peak is within the main beam of the copolar pattern but slightly offset and about 24 dB below the copolar main lobe. The "non-radiating" sides of patches cause this cross-pol lobe. This low separation between the copolar and cross-polar peaks would cause significant bias in case of SHV polarimetric mode. But if the AHV mode or SHV with phase coding (to suppress bias first order couplings) are used the 24 dB isolation

would be sufficient. Nonetheless, the rest of the radar hardware also can cause coupling plus the gains and phases in the H and V channels affect the values of the polarimetric variables. These facts could make calibration very challenging (i.e., correct determination of polarimetric variables).

For calculated radiation patterns, we can evaluate antenna induced polarimetric biases as function of angle. The cause of this bias is identified in the non-radiating sides of each patch element (cross-polar bias) and the geometrical projection of fields (geometrical bias). Following the research in determining the causes of the observed differential phase and Z_{DR} bias [14] we calculated the differential phase and differential gain that were observed by TPD in light rain (zenith pointing). The differential gain biases the Z_{DR} and the system differential phase introduces an offset to the measured differential phase. These biases are intrinsic to the system (antenna and radar together). Depending on the intended polarization, the calculated fields determine the copolar or cross-polar radiation pattern of the antenna. For each of the beam direction we obtain horizontal and vertical component of the field. These components are out of phase resulting in elliptical polarization for either of the ports excited. For this general case knowing the components and their phase difference we can calculate the tilt of the polarization ellipse ψ. In case of a vertically oriented panel and exitation of the port for the intended horizontal polarizaiotn this angle is

$$\psi = \frac{1}{2}\arctan\left(\frac{2F_{hv}F_{vv}}{F_{vv}^2+F_{hv}^2}\cos[\measuredangle(F_{vv}) - \measuredangle(F_{hv})]\right), \tag{14}$$

where ψ depends on the pointing direction (θ_0, ϕ_0) and the F_{ij}s are values of (6) at beam center.

The differential gain is

$$G_{dif} = g_h(\text{dB}) - g_v(\text{dB}). \tag{15}$$

The antenna can also create differential phase between the horizontally and vertically oriented fields,

$$\Phi_{Tx} = \arg(F_{vv}) - \arg(F_{hh}) \tag{16}$$

Angular dependences of the differential phase and gain of the TPD as function of beam pointing direction in the horizontal principal plane are plotted in Fig. 6. The values in Fig. 6 are calculated for the antenna without radome cover (blue) and with radome cover (red). The differential phase (Fig. 6 left) for the TPD antenna with the radome cover exhibits significant change. The dependence is similar to the one observed at zenith pointing measurements [14]. Note that the phases in Fig. 6 are one-way, while the total differential phase affecting measurements is the two-way (transmit and receive) value. In general, transmission and reception antenna effects are not identical (i.e., there can be taper on reception) thus should be calculated separately.

Differential phase variation of the TPD antenna is on the order of 2 to 3^o and is due to the change in the phase center position while beam steering. With the radome the differential phase increases to about 26^o. This significant difference is caused by the reflection mechanism that is not the same for both polarizations. While the vertically (V) polarized fields have parallel incidence to the radome, the horizontally (H) polarized fields have oblique incidence as the beam is steered in the horizontal plane.

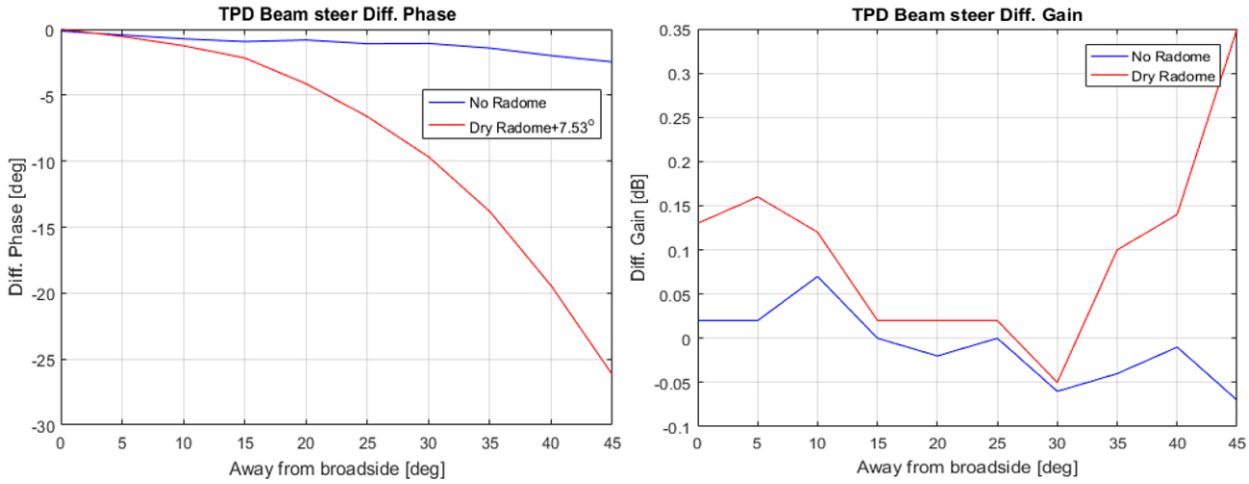

Fig. 6. Differential phase and differential gain calculated at the beam peak for the TPD antenna as function of beam position. Curves in blue represent the values for the antenna without radome whereas the red curves represent values with for the radome covered antenna

5. Conclusions

Determination of the polarimetric variables on weather radars with planar phased array antennas is challenging. Thus far no one has demonstrated a viable approach on a real system. The estimates of these variables depend on the beam pointing direction. For vertically oriented arrays with good cross-polar isolation and beam pointing in the principal planes the returns are not coupled. This significantly simplifies computation of the polarimetric variable although determining the transfer functions for the two polarization channels is still required. These depend on the transmitter and receiver and antenna gains.

At pointing directions out of the principal planes the equations relating powers and correlations of the received voltages are coupled and the coupling coefficients are functions of the antenna patterns. For large arrays the antenna parameters are hard to measure with the precision required for computation of the polarimetric variables. In such cases the tools of computational electromagnetics can be applied to simulate (determine) the patterns at the various polarizations.

We have applied the WIPL-D software to computation of copolar and cross-polar patterns of a relatively large (640 elements 2 m wide 0.8 m high) phased array antenna. The computed patterns agree with theoretical expectations. At broad side within the main beam the cross-polar patterns have four symmetric peaks each more than 50 dB below the main lobe maximum. In the principal plane two peaks remain within the main lobe and they are 40 dB below the main lobe peak. Out of the principal plane only one peak of the cross-polar pattern remains and at one pointing direction it is about 24 dB weaker than the main lobe peak. From the values of antenna gains at beam center it is possible to compute the axis of the polarization ellipse.

References

1. Sensi, J. Jr., 1988: The aegis system. Chapter 3 in “Aspects of modern radar”. Editor E. Brookner, Artech House, Norwood, MA.

2. Zrnic, D.S., J. F. Kimpel, D. E. Forsyth, A. Shapiro, G. Crain, R. Ferek, J. Heimmer, W. Benner, T. J. McNellis, and R. J. Vogt, 2007: Agile-beam phased array radar for weather observations. *Bull. Amer. Meteor. Soc*., **88,** pp. 1753–1766.

3. Weber, M. E., J.Y.N. Cho, J.S. Herd, J.M. Flavin, W.E. Benner, and G.S. Torok, 2007: The next-generation multimission U.S. surveillance radar network. *Bulletin of the Amer. Meteor. Soc*., 88**,** pp.1739-1752.
4. Sandifer, J. B., 2005: Meteorological measurements with a MWR-05XP phased array radar. MS Thesis, available at Calhoun: Institutional Archive of the Naval Postgraduate School. p 79
5. Salazar J. L., E. J. Knapp, R. H. Medina, A. P. Hopf, and D. J. McLaughlin, 2010: Scanning Performance of the CASA Solid State Phase-Tilt Radar Antenna Array. IEEE Inter. Symp. on Phased Array Systems and Technology., 8pp.
6. Zhang, G., R. J. Doviak, D. S. Zrnić, R. Palmer, Lei Lei, and Y. Al-Rashid, 2011: Polarimetric Phased-Array Radar for Weather Measurement: A Planar or Cylindrical Configuration? *Jo. Oceanic and Atmos. Tech.*, **28,** pp. 63-73.
7. Fulton, C., J. Salazar, D. Zrnic, D. Mirkovic, I. Ivic and D. Doviak, "Polarimetrie phased array calibration for large scale multi-mission radar applications," *2018 IEEE Radar Conference (RadarConf18)*, Oklahoma City, OK, 2018, pp. 1272-1277. doi: 10.1109/RADAR.2018.8378746
8. Zrnic, D.S., V.M. Melnikov, R.J. Doviak, and R. Plamer, 2015: Scanning Strategy for the Multifunction Phased-Array Radar to Satisfy Aviation and Meteorological Needs. *IEEE Geosci, Remote Sens. Letters,* **12,** 1204 – 1208.
9. Torres, S., R. Adams, C. D. Curtiw, E. Forren, D. E. Forsyth, I. R. Ivic D. Priegnitz, J Thomson, and D. A. Warde, 2016: Adaptive –weather surfeilllance and multifunction capabilities of the National Weather Radar Testbed Phase array radar. *Proc. IEEE*, **104,** pp. 660-672.
10. Fulton, C., M. Yeary, D. Thompson, J. Lake, and A. Mitchell, 2016: "Digital phased arrays: Challenges and opportunities," *Proceedings of the IEEE*, **104**, pp. 487–503.
11. Crain, G.E., and D. Staiman, 2009: "Polarization selection for phased array weather radar" *IIPS for Meteorology, Oceanography, and Hydrology, 25th Int. Conf. on,* New Orleans, AMS.
12. Doviak, Richard J., and Dusan S. Zrnic. *Doppler Radar & Weather Observations*. Dover, 2006.
13. Zrnić, D. S., R. J. Doviak, G. Zhang, and R.V. Ryzhkov, 2010: Bias in differential reflectivity due to cross-coupling through the radiation patterns of polarimetric weather radars. *J. Atmos. Oceanic Technol*., **27**, 1624-1637.
14. Mirkovic, D., & Zrnic, D. S. (2018). Polarimetric calibration using the computational electromagnetic approach. *2018 IEEE Radar Conference (RadarConf18)*, (pp. 1348-1352). Oklahoma City. doi:10.1109/RADAR.2018.8378760
15. WIPL-D. (2019). *WIPL-D Pro EM solver*. (WIPL-D d.o.o) Retrieved 2 28, 2019, from www.wipl-d.com
16. Ludwig, A. C. (1973The Definition of Cross Polarization. *IEEE Trans. on Ant. and Prop.* (January), 116-119.).